



An Efficient Plant Disease Detection: Possibility Neutrosophic Hypersoft Set Approach with Whale Optimization Algorithm

Abdalla Ibrahim Abdalla Musa^{1*}, Mohammed Abdullah Al-Hagery¹

¹Department of Computer Science, College of Computer, Qassim University, Buraydah, Saudi Arabia

Emails: ab.musa@qu.edu.sa; hajry@qu.edu.sa

Abstract

Indian agriculture aims at achieving sustainable development, which increases crop production per square unit without damaging the ecosystem and natural resources. Timely and prompt diagnosis and analysis of plant diseases are very beneficial in increasing food crop productivity and plant health and decreasing plant diseases. Plant disease specialists are not accessible in distant regions therefore there is an urgent need for reliable, automatic low-cost, and approachable solutions to detect plant disease without the expert's opinion and laboratory inspection. Classical machine learning (ML)-based image classification techniques and Deep learning (DL)-based computer vision (CV) approaches such as Convolutional Neural Networks (CNN) was employed to detect plant disease. Neutrosophic set (NS), a generality of fuzzy set (FS) and intuitionistic FS (IFS), presented to characterize inconsistent, uncertain, imprecise, and incomplete data in realistic conditions. Besides, interval NS (INSs) was exactly proposed to resolve the problems with a collection of numbers in the actual entity. On the other hand, there are high levels of operational reliability for INSs, along with the decision-making method and INS aggregation operators. This study presents an Efficient Plant Disease Detection using the Possibility Neutrosophic Hypersoft Set Approach (EPDD-pNSHSS) method. The suggested EPDD-pNSHSS method uses the DL method for the recognition and classification of plant diseases. Initially, the EPDD-pNSHSS method takes place the Median filtering (MF) through the preprocessing to progress image superiority and eliminate noise. In the meantime, the possibility neutrosophic hypersoft set (pNSHSS) classifier is utilized for the detection of diseased and healthy leaf images. To optimize the detection accuracy of the pNSHSS mechanism, the whale optimization algorithm (WOA) is employed for adjusting the hyperparameter value of the DSAE technique. Wide-ranging experiments are implemented to exhibit the supremacy of the EPDD-pNSHSS method. The empirical findings showcased the development of the EPDD-pNSHSS method over other existing techniques.

Keywords: Neutrosophic Hypersoft Set, Neutrosophic Logic; Whale Optimization Algorithm, Plant Disease Detection, Median Filtering

1. Introduction

Neutrosophic Logic (NL) is a new research field that every proposition has been projected to have the truth proportion in a sub-set T, the uncertainty proportion in a sub-set I, and the falsity proportion in a subset F [1]. We apply a sub-set of truth or falsity or indeterminacy, rather than a number because in several conditions we are unable to determine the proportions of falsity and truth but can only estimate them [2]. The sub-sets are not effective intervals but any sets (closed or open half-open intervals, constant, intersections, unions or discrete of the preceding sets, etc.) are maintained with the specified proposition. FS has a novel feature in the theory of the conventional set model [3]. Farming is one of the vital financial activities of the Indian sub-continent and two-thirds population is directly concerned with agricultural and related work [4]. The farming region desires additional improvement owing to variations in economic and weather conditions in the country. The harvests must be healthy to get additional valuable outcomes [5]. Crop illness is a reason for reducing the quality and quantity of harvests in the lands. Enormous insecticides are accessible to reduce the illnesses of the farming harvests to increase crop production in the lands [6]. Crop waste is rising owing to illnesses, so it is important to recognize the illnesses timely and precisely [7].

In a developing country, specifically in South Asia, many people depend on farming indirectly or directly [8], it is becoming significant in such countries to utilize the application-based plant illness classification that can support cultivators in identifying the reason for illnesses and make the safety measure to treat them [9]. Early detection of plant illnesses based on their color, growth, size of the model, etc. will be useful to the cultivators. A simple application will be useful for the farmers to work on individual image-based disease recognition [10]. To execute the farming procedures, conventional ML methods are used in several types of research [11]. But, in recent times, DL as a subset of ML, is extremely effective for real object detection, classification, and detection reasons [12]. Numerous advanced DL methods are used to execute plant illness identification by utilizing known DL structures [13]. Additionally, many scientists proposed a revised version of DL methods to increase the disease classification performance in various kinds of plants. Some notable researches are emphasized in this sector [14]. For instance, the latest study offered a comparative analysis of several CNN and DL optimizations to achieve the best outcomes for plant illness identification. The research introduced a CNN method to identify illness in tea plants. One more research was performed to introduce the dual-modified versions of MobileNet methods for the identification of numerous plant illnesses [15].

This study presents an Efficient Plant Disease Detection using the Possibility Neutrosophic Hypersoft Set Approach (EPDD-pNSHSS) method. The suggested EPDD-pNSHSS method uses the DL method for the recognition and classification of plant illnesses. Initially, the EPDD-pNSHSS method takes place the Median filtering (MF) through the preprocessing to progress image superiority and eliminate noise. Meanwhile, the possibility neutrosophic hypersoft set (pNSHSS) classifier is utilized for the detection of diseased and healthy leaf images. To optimize the detection accuracy of the pNSHSS mechanism, the whale optimizer algorithm (WOA) is used for adjusting the hyperparameter value of the DSAE technique. The empirical findings showcased the development of the EPDD-pNSHSS method over other existing techniques.

2. Related Works

Radočaj et al. [16] introduced a flexible component built on the function of Mish activation, Batch normalization (IncMB) and the Inception module is one of deep neural network (DNN). A CNN with transfer learning (TL) has been utilized as the baseline for measured methods for tomato illness recognition: CNN by IncMB component, CNN, and CNN with a support vector machine (SVM). Chug et al. [17] proposed a new model that integrates the improvements of both DL and ML. The developed model contains forty various Hybrid DL methods that contain the integration of 8 various versions of pre-trained DL structure, viz., EfficientNet (B0toB7) as feature extractors and 5 ML methods, i.e., AdaBoost, Logistic Regression (LR), k-Nearest Neighbors (kNN), Stochastic Gradient Boosting (SGB) and Random Forest (RF), as classifiers. The Optuna method was utilized in recent research to enhance the hyper-parameters of these classifiers. In [18], a new DAE-Mask technique that depends on edge and diversification-augmented features was developed. DAE-Mask utilized a Densely Connected Convolutional Network (DenseNet) for the initial, and backbone feature extractions system relating Feature Pyramid Networks (FPNs) and attention mechanism has been created to remove the diversification-augmented feature. To speed up DAE-Mask, an Edge Agreement Head modulus depends on the Sobel filter is aimed to equate the edge feature through training that developed the model's mask generation productivity.

Ullah et al. [19] introduced a hybrid DL-based method to identify tomato plant illnesses with leaf imageries. To complete this task, this research shows the combination of 2 pre-trained methods, such as MobileNet and EfficientNetB3 (EffiMob-Net) to identify tomato leaf illnesses precisely. Additionally, model overfitting was addressed by several methods, like dropout, batch normalization (BN), and regularization. Hyper-parameter fine-tuning was executed to select the optimum parameter for developing the suitable method. Nawaz et al. [20] concentrated on overcoming the stated limits by developing a new and effectual DL method named CoffeeNet. Explicitly, a developed CenterNet method is presented by initiating the spatial-channel attention strategy-based ResNet50 method for the estimation of depth and illness-exact model features which are categorized by the one-step detector of the CenterNet method. Jerome et al. [21] propose a DL based Assessment-based CNN (A-CNN) technique. To improve the excellence of plant imageries and obtain a smooth look, an Improved Gaussian Wiener Filter (OGWF) is used for image pre-processing. Moreover, the edge of plant leaves could be identified by applying canny and Sobel operatives. Next, Otsu's Threshold Fragment (OTF) method is used for seperating the illness affected area. Furthermore, the Spatial Grey-Level Dependence Matrix (SGLDM) method has been used to detect the appropriate features of the affected leaf.

3. The Proposed Model

In this paper, we presented a novel EPDD-pNSHSS technique. The suggested EPDD-pNSHSS method uses the DL method for the recognition and classification of plant illnesses. The EPDD-pNSHSS technique comprises MF-based pre-processing, pNSHSS-based detection of diseased, and WOA-based hyperparameter tuning. Figure 1 portrays the complete workflow of EPDD-pNSHSS model.

A. Image Preprocessing

Initially, the EPDD-pNSHSS method takes place the MF through preprocessing to improve image quality and eliminate noise. The MF model is a critical preprocessing stage in plant disease recognition, to successfully eliminate noises from an image [22]. By exchanging every pixel values with the median value of adjacent pixels, this nonlinear filter method retains edges while eradicating random variation, which ensures a more accurate and clearer examination of plant disease symptoms. This improves the consistency of succeeding image processing tasks namely classification and segmentation.

B. Disease Detection using pNHSS Classifier

Next, the pNSHSS classifier is employed for the detection of diseased and healthy leaf images. The pNHs-set classifier is employed for the strong identification and detection of cyber threats [23].

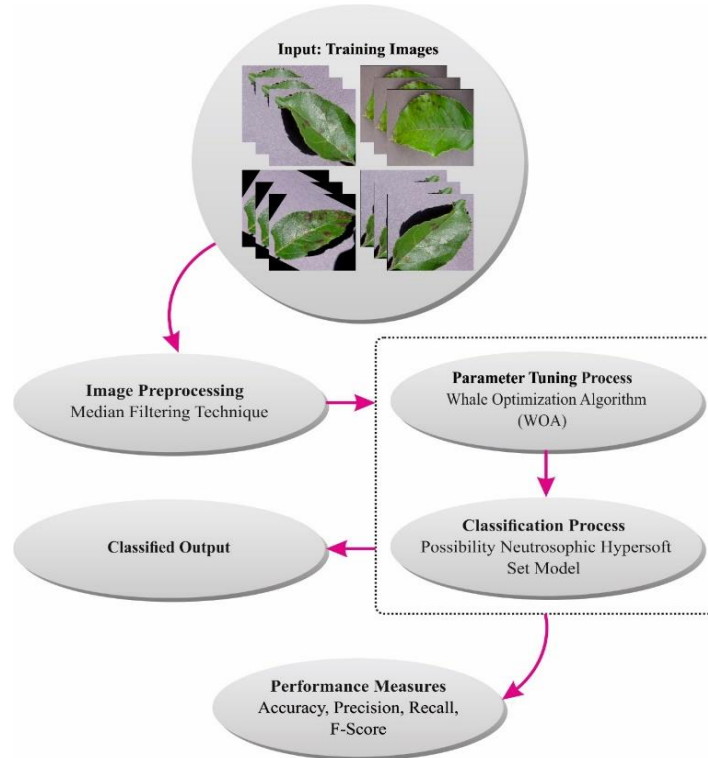


Figure 1. Overall flow of EPDD-pNSHSS method

The Hs-set over Z represents couples $(\mathcal{W}, \mathcal{H})$, \mathcal{H} denotes the Cartesian product of $\mathcal{H}^i, i = 1, 2, 3, \dots, n, \mathcal{H}^i \cap \mathcal{H}^j = \emptyset$ for $i \neq j$ encompassing characteristics value $\hat{a}_i = 1, 2, 3, \dots, n, \hat{a}_i \neq \hat{a}_j, i \neq j$, correspondingly. Each $\mathcal{W}(\hat{h}_\alpha), \alpha = 1, 2, 3, \dots, k$ characterizes the subset of Z and is identified as a multi-argument assessed component of Hs-set $(\mathcal{W}, \mathcal{H})$. As well, a Hs-set $(\mathcal{W}, \mathcal{H})$ is realized as a parameter range of the initial universe Z .

The Hs-set $(\mathcal{W}, \mathcal{H})$ is named a fuzzy Hs-set. If $\mathbb{P}(Z)$ in $W: H \rightarrow \mathbb{P}(Z)$ is substituted by the $F(Z), IF(Z)$ and $M(Z)$, while $F(Z), IF(Z)$ and $N(Z)$ are corresponding relationships of FS, IFS, and NS on Z .

A pNs-set \mathfrak{R}_s is given as follows

$$\mathfrak{R}_s = \{(\zeta_s(\hat{a})\psi_s(\hat{a}), \zeta_s(Z) \in \mathbb{N}\psi_s(a) \in \mathbb{F}(Z) \text{ and } \hat{a} \in \mathbb{A}) \text{ whereas } \mathbb{A} \subseteq \mathbb{E} \text{ (a parameter set), } \zeta_s: \mathbb{A} \rightarrow \mathbb{N} \text{ and } \psi_s: \mathbb{A} \rightarrow \mathbb{F}(Z)\}.$$

This portion offers the set-theoretic processes and description of the pNHs-set with scientific instance. It is an element of the widespread view in any employment procedure, a board is produced to discuss the investigated interviewees at first. This board generally has a leader and other participants, who know the explicit field. All follower groups of the panel are concentrated on calculating the fitness and ability of the interviewees. Numerous involved provide their proficient views in 3D, viz., mention, remove, or be neutral about the assessment of the candidate's equivalent to multi-argument collections. The leader is approved to inspect the proficient opinions with the approval stage. Briefly, 3 circumstances in this situation must be confronted with a particular technique:

1. The situation shapes the dynamic detection into their interrelated sub-parametric value in the process of dissimilar sets.
2. The circumstance requires the assertion of the *maa*-function is capable of undertaking the multi-argument area.
3. The condition that requires the decision-makers to offer their skilled decisions in the procedure of neutrosophic value that assurance the 3D.
4. The condition requires the prospect grade reflection to evaluate the recognition stage of the specialized choices.

The study is not enough to transport any mathematical technique to encounter all the aforementioned situations in a single technique. This continues to be the motivation of this investigation. The established technique *pNHS*-set, is proficient of handling the abovementioned conditions as solitary architecture. The *pNHS*-set contains of 3 different fragments namely possibility-degree-based set, HS, and NS. The *pNHS*-set accomplishes conditions 1 and 2 through the HS; circumstance 3 is endeavoured through the NS; the last circumstance 4 is controlled via the possibility-degree-based set. Many states of realism are available such as risk analysis, project selection, medical analysis, and product selection, and several need the situation of *pNHS*.

The *pNHS*-set $\mathfrak{F}\psi$ over hyper slot universe (Z, J) is the set $\psi = \left\{ \left(\delta, \left\{ \left(\frac{\hat{z}}{F(\delta)(\hat{z})}, \psi : Z \in Z \right) \right\} : \delta \in J \right\}$ while J_i represents the non-overlapping parameter set $a_{it} \ i = 1_t 2_t \dots$, as $(J_1 \times J_2 \times \dots \times J_n, F_\psi : J \rightarrow \mathbb{N}_z \times I_z, \mathfrak{F} : J \rightarrow \mathbb{N}_z, \psi : J \rightarrow I_z, I_z \in F(Z)$, and $\mathbb{N}_z \in \mathbb{N}(Z)$, correspondingly; $\mathfrak{F}(\delta)(\hat{z})$ is the NS value of $\hat{z} \in Z$ in $F(\delta)$, and $\psi(\delta)(\hat{z})$ is the probable grade of $\hat{z} \in Z$ in $F(\delta)$. So, $F_\psi(\delta_i)$ is given as follows:

$$\mathfrak{F}_\psi(\delta_i) = \left\{ \left(\frac{\hat{z}}{\mathfrak{F}(\delta_i)(\hat{z}_1)}, \psi(\delta_i)(\hat{z}) \right), \left(\frac{\hat{z}}{\mathfrak{F}(\delta_i)(\hat{z})}, \psi(\delta_i)(\hat{z}) \right), \dots, \left(\frac{\hat{z}}{\mathfrak{F}(\delta_i)(\hat{z})}, \psi(\delta_i)(\hat{z}) \right) \right\}$$

For availability, the *pNHS*-set is F_ψ and Ω_{pnhss} is the family.

Consider the healthcare manager of a public sanatorium produces a group encompassing emotion professionals to evaluate sentiment disorders by identifying proper parameters. The 4 classes of sentiment disorders are considered enclosed in discourse set $Z = \{\hat{D}_1, \hat{D}_2, \hat{D}_3, \hat{D}_4\}$. The group members a parametric set $a_1 =$ chest pain type, $a_2 =$ resting blood pressure (mmHg), and $a_3 =$ serum cholesterol (*mg/dL*) with the collective agreement. When the perfect investigation, the parameter is characterized into the connected parameter set is $J_1 = \{a_{11} = \text{typicalangina}, a_{12} = a \text{Typicalangina}\}_t J_2 = \{a_{21} = 150_t a_{22} = 180\}$, and $J_3 = \{a_{31} = 320\}$, correspondingly. To get the parametric tuples, the Cartesian product was evaluated by $J_1 \times J_2 \times J_3 = \{\delta_1, \delta_2, \delta_3, \delta_4\}$. The connections are concentrated to distribute the opinions in the technique of NS components via the parametric tuple's presence. The conventional thought is composed of multi-argument projected fundamentals of *pNHS*-sets that are considered in the following:

$$\begin{aligned} \mathfrak{F}_\psi(\delta_1) &= \left\{ \left(\frac{\hat{D}_1}{\langle 0.3, 0.1, 0.2 \rangle}, 0.2 \right), \left(\frac{\hat{D}_2}{\langle 0.4, 0.2, 0.3 \rangle}, 0.3 \right), \left(\frac{\hat{D}_3}{\langle 0.5, 0.3, 0.4 \rangle}, 0.4 \right), \left(\frac{\hat{D}_4}{\langle 0.6, 0.4, 0.5 \rangle}, 0.5 \right) \right\} \\ F_\psi(\delta_2) &= \left\{ \left(\frac{\hat{D}}{\langle 0.7, 0.2, 0.3 \rangle}, 0.8 \right), \left(\frac{\hat{D}_2}{\langle 0.6, 0.3, 0.4 \rangle}, 0.8 \right), \left(\frac{\hat{D}_3}{\langle 0.6, 0.4, 0.5 \rangle}, 0.7 \right), \left(\frac{\hat{D}_4}{\langle 0.5, 0.5, 0.6 \rangle}, 0.6 \right) \right\} \\ F_\psi(\delta_3) &= \left\{ \left(\frac{\hat{D}_1}{\langle 0.5, 0.1, 0.1 \rangle}, 0.1 \right), \left(\frac{\hat{D}_2}{\langle 0.4, 0.1, 0.2 \rangle}, 0.2 \right), \left(\frac{\hat{D}_3}{\langle 0.5, 0.1, 0.3 \rangle}, 0.3 \right), \left(\frac{\hat{D}_4}{\langle 0.6, 0.2, 0.4 \rangle}, 0.4 \right) \right\} \\ F_\psi(\delta_4) &= \left\{ \left(\frac{\hat{D}_1}{\langle 0.7, 0.1, 0.2 \rangle}, 0.2 \right), \left(\frac{\hat{D}_2}{\langle 0.5, 0.1, 0.3 \rangle}, 0.3 \right), \left(\frac{\hat{D}_3}{\langle 0.6, 0.4, 0.4 \rangle}, 0.4 \right), \left(\frac{\hat{D}_4}{\langle 0.7, 0.2, 0.5 \rangle}, 0.5 \right) \right\} \end{aligned}$$

Next, \mathfrak{F}_ψ symbolizes a *pNHS*-set over (J) . It is the matrix representation as:

$$F_\psi = \begin{pmatrix} (\langle 0.3, 0.1, 0.2 \rangle, 0.2) & (\langle 0.4, 0.2, 0.3 \rangle, 0.3) & (\langle 0.5, 0.3, 0.4 \rangle, 0.4) & (\langle 0.6, 0.4, 0.5 \rangle, 0.5) \\ (\langle 0.7, 0.2, 0.3 \rangle, 0.8) & (\langle 0.6, 0.3, 0.4 \rangle, 0.8) & (\langle 0.6, 0.4, 0.5 \rangle, 0.7) & (\langle 0.5, 0.5, 0.6 \rangle, 0.6) \\ (\langle 0.5, 0.1, 0.1 \rangle, 0.1) & (\langle 0.4, 0.1, 0.2 \rangle, 0.2) & (\langle 0.5, 0.1, 0.3 \rangle, 0.3) & (\langle 0.6, 0.2, 0.4 \rangle, 0.4) \\ (\langle 0.7, 0.1, 0.2 \rangle, 0.2) & (\langle 0.5, 0.1, 0.3 \rangle, 0.3) & (\langle 0.6, 0.4, 0.4 \rangle, 0.4) & (\langle 0.7, 0.2, 0.5 \rangle, 0.5) \end{pmatrix}$$

In this work, the initial element $(\langle 0.3, 0.1, 0.2 \rangle, 0.2)$ specifies that every decision-makers have together transported the degree as 0.3 (30%), indeterminate degree as 0.1(10%), and non-membership degree as 0.2 (20%)

for a disorder D_1 , and a probability function of 0.2 (20%) is distributed through the leader for the professional thoughts approval $\langle \langle 0.3, 0.1, 0.2 \rangle, 0.2 \rangle$ to D_1 by limiting in estimation δ_1 . Similarly, other assessed backgrounds and their value are considered in a parallel technique.

Consider that $\mathfrak{A}_\psi \mathfrak{B}_\zeta \in \Omega_{pnhss}$ then:

- (i) $\mathfrak{A}_\psi \cup \mathfrak{B}_\zeta$ represents a pNHs-set C_v with $C(\delta) = \{\mathfrak{A}(\delta), \mathfrak{B}(\delta)\}$, and $v(\delta) = \max\{\psi(\delta), \zeta(\delta)\}$.
- (ii) $\mathfrak{A}_\psi \cap \mathfrak{B}_\zeta$ denotes the pNHs-set \mathfrak{D}_ω with $\mathfrak{D}(\delta) = \Pi\{\mathfrak{A}(\delta), \mathfrak{B}(\delta)\}$, and $\omega(\delta) = \min\{\zeta(\delta)\}$. Let \sqcup is a union and \cap be the intersection of NS, correspondingly.

Consider the statistics from Instance 1, dual pNHs-set $\mathfrak{A}_\psi \mathfrak{B}_\zeta \in \Omega_{pnhss}$ are constructed whose matrix representation is given as follows:

$$\mathfrak{A}_\psi = \begin{pmatrix} \langle \langle 0.1, 0.2, 0.3 \rangle, 0.2 \rangle & \langle \langle 0.2, 0.3, 0.4 \rangle, 0.3 \rangle & \langle \langle 0.3, 0.4, 0.5 \rangle, 0.4 \rangle & \langle \langle 0.4, 0.5, 0.6 \rangle, 0.5 \rangle \\ \langle \langle 0.5, 0.5, 0.6 \rangle, 0.8 \rangle & \langle \langle 0.6, 0.4, 0.5 \rangle, 0.8 \rangle & \langle \langle 0.7, 0.3, 0.4 \rangle, 0.7 \rangle & \langle \langle 0.9, 0.1, 0.2 \rangle, 0.6 \rangle \\ \langle \langle 0.4, 0.3, 0.4 \rangle, 0.1 \rangle & \langle \langle 0.6, 0.4, 0.5 \rangle, 0.2 \rangle & \langle \langle 0.7, 0.2, 0.3 \rangle, 0.3 \rangle & \langle \langle 0.4, 0.1, 0.2 \rangle, 0.4 \rangle \\ \langle \langle 0.6, 0.2, 0.3 \rangle, 0.2 \rangle & \langle \langle 0.7, 0.3, 0.4 \rangle, 0.3 \rangle & \langle \langle 0.5, 0.2, 0.3 \rangle, 0.4 \rangle & \langle \langle 0.7, 0.2, 0.3 \rangle, 0.5 \rangle \end{pmatrix}$$

and

$$\mathfrak{B}_\zeta = \begin{pmatrix} \langle \langle 0.2, 0.1, 0.2 \rangle, 0.3 \rangle & \langle \langle 0.3, 0.2, 0.3 \rangle, 0.4 \rangle & \langle \langle 0.4, 0.3, 0.4 \rangle, 0.5 \rangle & \langle \langle 0.5, 0.4, 0.5 \rangle, 0.6 \rangle \\ \langle \langle 0.6, 0.4, 0.5 \rangle, 0.9 \rangle & \langle \langle 0.7, 0.3, 0.4 \rangle, 0.9 \rangle & \langle \langle 0.8, 0.2, 0.3 \rangle, 0.8 \rangle & \langle \langle 1.0, 0.0, 0.1 \rangle, 0.7 \rangle \\ \langle \langle 0.5, 0.2, 0.3 \rangle, 0.2 \rangle & \langle \langle 0.7, 0.3, 0.4 \rangle, 0.3 \rangle & \langle \langle 0.8, 0.1, 0.2 \rangle, 0.4 \rangle & \langle \langle 0.5, 0.0, 0.1 \rangle, 0.5 \rangle \\ \langle \langle 0.7, 0.1, 0.2 \rangle, 0.3 \rangle & \langle \langle 0.8, 0.2, 0.3 \rangle, 0.4 \rangle & \langle \langle 0.6, 0.1, 0.2 \rangle, 0.5 \rangle & \langle \langle 0.8, 0.1, 0.2 \rangle, 0.6 \rangle \end{pmatrix}$$

Then $C_v = \mathfrak{A}_\psi \cup \mathfrak{B}_\zeta = \mathfrak{B}_\zeta$ and $\mathfrak{D}_\omega = \mathfrak{A}_\psi \cap \mathfrak{B}_\zeta = \mathfrak{A}_\psi$.

3.3. Hyperparameter Tuning using WOA

WOA is nothing but an optimizer method, which is stimulated by humpback whales [24]. When they determine their objective, humpback whales can enclose it. The WOA technique functions below the principle that the existing finest candidate solution is the victim of notice or nearby to the optimum. Since, the position of the optimum project in the searching space is a preceding mysterious. After the finest searching agent is nominated, the residual searching agents will try to appeal nearer to it.

The behavior of whales was established in the below mentioned formulations:

$$D = |C \cdot X^*(t) - X(t)| \quad (1)$$

$$X(t+1) = X^*(t) - A \cdot D \quad (2)$$

Whereas t signifies the existing iteration, X^* embodies the location vector of the finest result, A , and C refers to the vector of coefficient, $\|$ signifies the absolute value, X indicates the location vector, and (\cdot) denotes element-wise multiplication. It is vital to retain that if a superior solution arises after every cycle, X^* must be altered. A and C vectors are intended to utilize the Eqs. (1-2).

Bubble-Net-Attack Method (Exploitation Stage)

Dual tactics were formed to exactly pretend the humpback behavior of whales in bubble nets:

1. Shrinking Encircling Mechanism

The mechanism of shrinking encircling is parallel to GWO (refer Eqs. (1) - (2)).

2. Spiral Upgrading Location

The initial stage is to define the space among the whale at the location (X, Y) and the prey at the location (X^*, Y^*) . A spiral calculation (Eq. (3)) is constructed among the whale location and its victim to emulate the spiral movement of humpback whales.

$$X(t+1) = D' \cdot \exp^{bl} \cdot \cos(2\pi l) + X^*(t) \quad (3)$$

Here, D' is signified in Eq. (4) and designates the space among the i th whale to the victim (finest solution attained to this point), b denotes a constant to define the logarithmic spiral shape, l represents the randomly generated values in $[-1$ and $1]$ and (\cdot) symbol refers to an element-wise multiplication.

$$D' = |X^*(t) - X(t)| \quad (4)$$

The humpback whales swim at the same time in a falling circle and helix shape near their victim. To describe this parallel behavior, we accept a 50% possibility of selecting both the shrinking encirclement device and the helix method to upgrade the whales' location. Furthermore, according to the bubble-net model, humpback whales search for victim randomly. The expression is given below.

Search for Prey (Exploration Stage)

Prey exploration is completed utilizing a similar method dependent upon an alteration to the A vector. It randomly hunt based on their locations. So, to strengthen the searching agent to travel from a position whale, A with a arbitrary value bigger or lesser than 1 was used. The searching agent location is upgraded depending upon an arbitrarily selected searching agent at the time of the exploration stage as different to the finest searching agent so far learned throughout the stage of exploitation. With help of this technique, $|A| > 1$ is a highlight exploration, so the WOA technique is capable of behavior a global searching. This stage is expressed mathematically as below:

$$D = |C \cdot X_{rand}(t) - X(t)| \quad (5)$$

$$X(t + 1) = X_{rand}(t) - A \cdot D \quad (6)$$

Here, X_{rand} signifies the randomly generated location vector selected from the existing population. Figure 2 depicts the flowchart of WOA.



Figure 2. Flowchart of WOA

The WOA method originates a FF to achieve amended classifier solution. It defines a positive number to denote the recovered efficiency of the candidate solution. In this paper, the reduction of the classifier rate of error is measured as FF and set in Eq. (7).

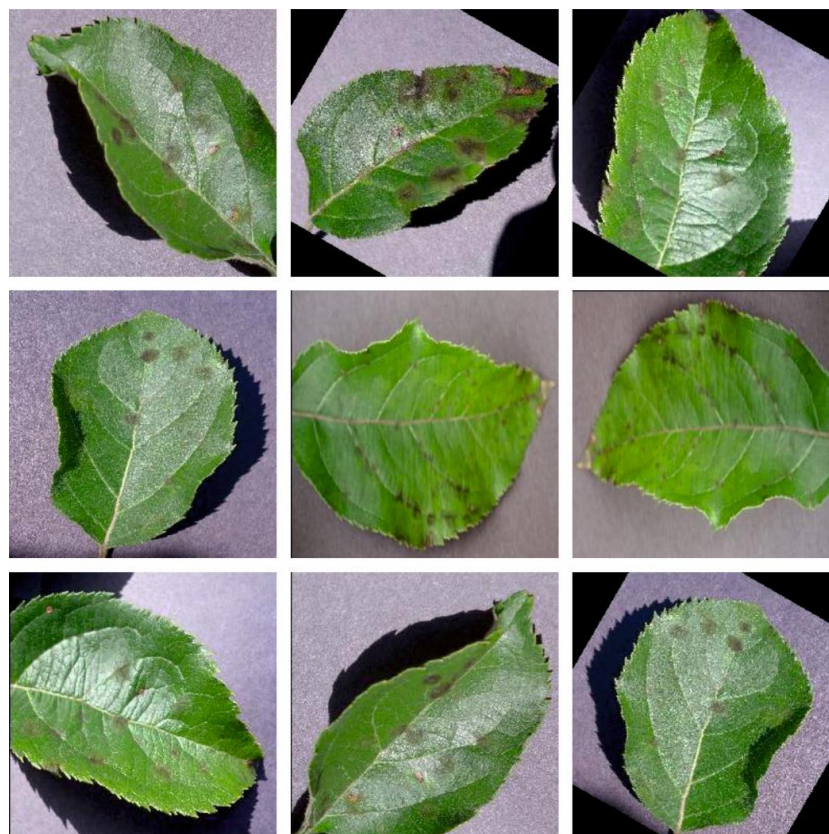
$$\begin{aligned} fitness(x_i) &= ClassifierErrorRate(x_i) \\ &= \frac{\text{no. of misclassified samples}}{\text{Total no. of samples}} * 100 \end{aligned} \quad (7)$$

4. Performance Validation

In this section, the experimental validation of the EPDD-pNSHSS technique is surveyed by using the apple plant illness dataset [25], which contains 7771 images with four classes as represented in Table 1. Figure 3 represents the sample imageries.

Table 1: Details on Dataset

Apple Plant Disease Dataset	
Disease	No. of Images
Scab	2016
Black Rot	1987
Cedar Apple Rust	1760
Healthy	2008
Total Images	7771

**Figure 3.** Sample images

In Table 2 and Figure 4, the plant disease detection outcomes of the EPDD-pNSHSS method with 70%TRAP and 30%TESP. The outcomes inferred that the EPDD-pNSHSS model has appropriately reached effective performances under four classes. With 70%TRAP, the EPDD-pNSHSS system offers average $accu_y$, $prec_n$, $reca_l$, F_{score} , and AUC_{score} of 96.04%, 91.98%, 91.96%, 91.97%, and 94.66%, respectively. Moreover, with 30%TESP, the EPDD-pNSHSS method provides average $accu_y$, $prec_n$, $reca_l$, F_{score} , and AUC_{score} of 96.38%, 92.60%, 92.55%, 92.57%, and 95.07%, respectively.

Table 2: Plant disease detection outcome of EPDD-pNSHSS method under 70%TRAP and 30%TESP

Classes	$Accu_y$	$Prec_n$	$Reca_l$	F_{score}	AUC_{score}
TRAP (70%)					
Scab	95.96	92.89	91.45	92.17	94.49
Black Rot	96.38	91.85	94.17	93.00	95.65
Cedar Apple Rust	94.63	88.85	87.57	88.21	92.15
Healthy	97.19	94.33	94.67	94.50	96.36
Average	96.04	91.98	91.96	91.97	94.66

TESP (30%)					
Scab	96.66	93.22	93.84	93.53	95.74
Black Rot	96.57	92.18	94.65	93.40	95.94
Cedar Apple Rust	94.94	89.26	87.52	88.39	92.28
Healthy	97.34	95.74	94.19	94.96	96.34
Average	96.38	92.60	92.55	92.57	95.07

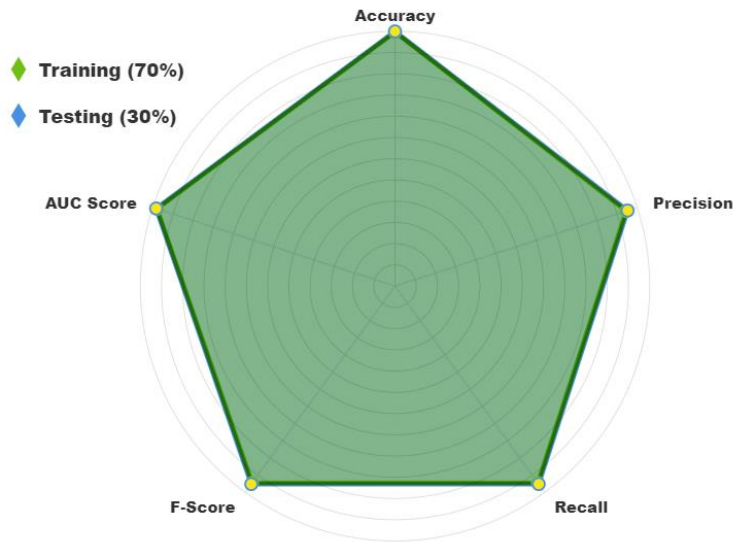


Figure 4. Average of EPDD-pNSHSS technique under 70% TRAP and 30% TESP

In Figure 5, the training and validation accuracy outcomes of the EPDD-pNSHSS method are established. The accuracy values are intended throughout 0-25 epochs. The result highlighted that the training and validation accuracy values show a rising tendency which alerted the ability of the EPDD-pNSHSS method with improved performance over many iterations. Moreover, the training and validation accuracy remains closer over the epochs, which defines the lowest nominal overfitting and shows an enhanced performance of the EPDD-pNSHSS method, assuring a steady forecast on unseen samples.

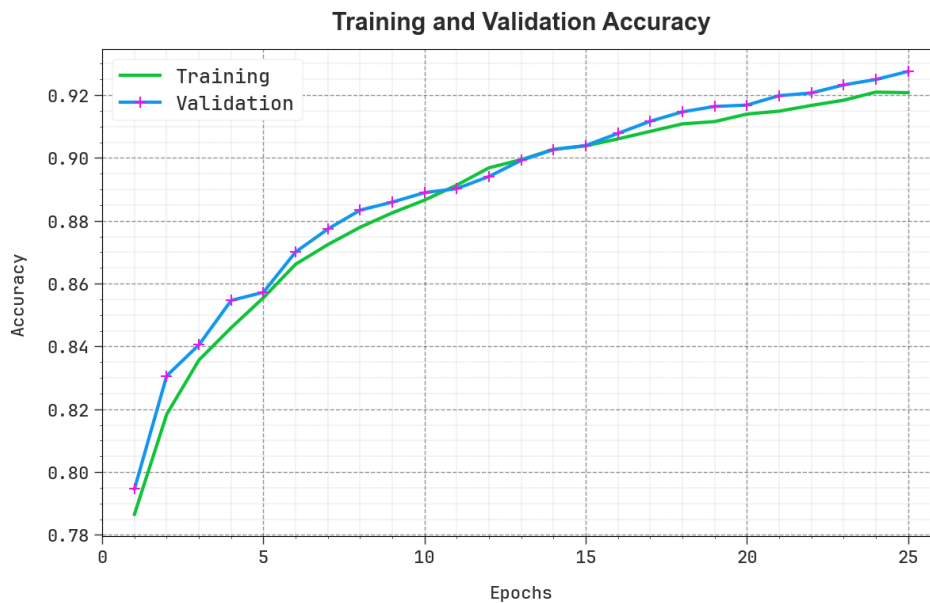


Figure 5. Accy, curve of EPDD-pNSHSS technique

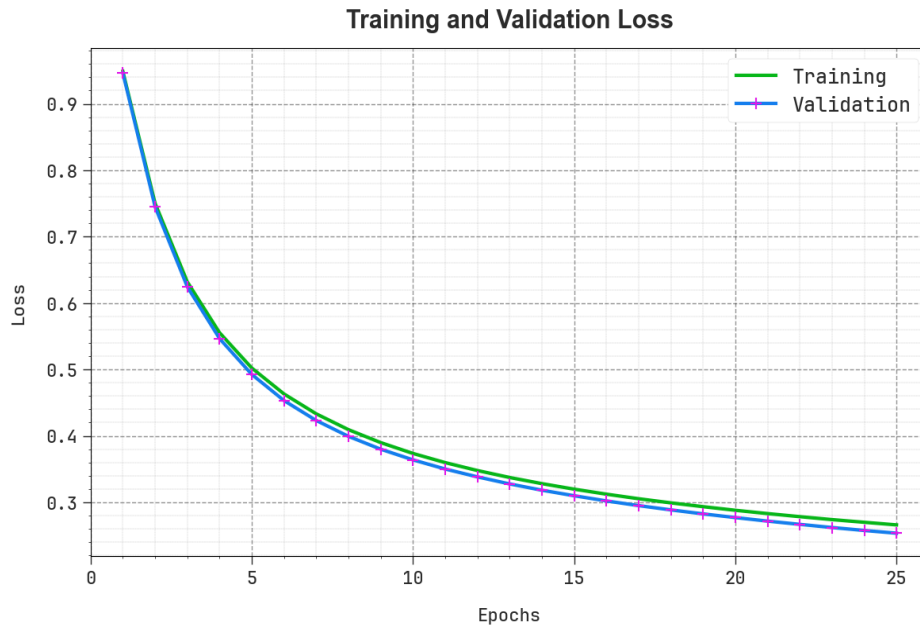


Figure 6. Loss curve of EPDD-pNSHSS technique

In Figure 6, the training and validation loss graph of the EPDD-pNSHSS technique is displayed. The loss values are calculated throughout 0-25 epochs. It is expressed that the training and validation accuracy values establish a declining tendency, which notified the ability of the EPDD-pNSHSS method to balance a trade-off between data fitting and generalization. The continual reduction in loss values also assures the amended performance of the EPDD-pNSHSS model and tunes the prediction results over time.

In Table 3 and Figure 7, the experimental results of the EPDD-pNSHSS model with current models are given [26]. The results exhibit that the BP and SVM models have shown worse performance with $accu_y$ of 54.63% and 68.73%. Simultaneously, the CNN-MobileNet and InceptionV3 approaches have obtained slightly increased outcomes with $accu_y$ of 73.50% and 75.59%, respectively. Besides, the ResNet152 and AlexNet models have attained moderately closer performance. Meanwhile, the RDODL-APDC model has resulted in considerable outcomes with $accu_y$ of 95.80%, respectively. But the EPDD-pNSHSS technique outperforms the other models with maximum $accu_y$ of 96.38%.

Table 3: Comparative outcome of EPDD-pNSHSS technique with other models

Method	$Accu_y$ (%)
EPDD-pNSHSS	96.38
RDODL-APDC	95.80
SVM Classifier	68.73
BP Algorithm	54.63
AlexNet Model	91.19
CNN-MobileNet	73.50
InceptionV3	75.59
ResNet152	77.65

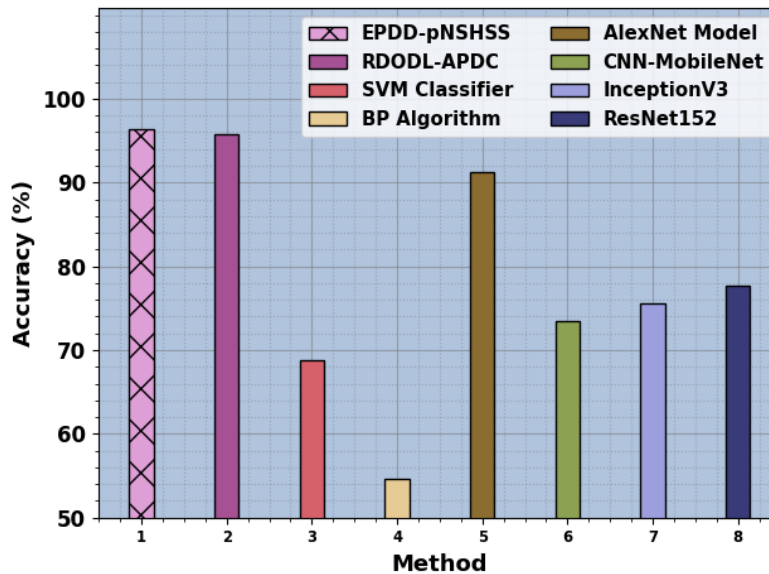


Figure 7. Comparative outcome of EPDD-pNSHSS method with recent techniques

5. Conclusion

In this research work, we have presented a novel EPDD-pNSHSS model. The presented EPDD-pNSHSS technique utilizes the DL method for the recognition and identification of plant diseases. Initially, the EPDD-pNSHSS model takes place the MF using the pre-processing to increase image superiority and eliminate noise. Furthermore, the pNSHSS classifier is employed for the recognition of unhealthy and healthy leaf imageries. To optimize the detection accuracy of the pNSHSS model, the WOA method is utilized for adjusting the hyperparameter value of the DSAE technique. Wide-ranging investigations are employed to exhibit the dominance of the EPDD-pNSHSS method. The empirical findings accentuated the development of the EPDD-pNSHSS method over other existing techniques.

Funding: “This research received no external funding”

Conflicts of Interest: “The authors declare no conflict of interest.”

References

- [1] Abobala, M., 2020. n-Cyclic Refined Neutrosophic Algebraic Systems Of Sub-Indeterminacies, An Application To Rings and Modules. *International Journal of Neutrosophic Science*, 12, pp.81-95.
- [2] Abobala, M., "Classical Homomorphisms Between Refined Neutrosophic Rings and Neutrosophic Rings", *International Journal of Neutrosophic Science*, Vol. 5, pp. 72-75, 2020.
- [3] Alhamido, R., and Abobala, M., "AH-Substructures in Neutrosophic Modules", *International Journal of Neutrosophic Science*, Vol. 7, pp. 79-86 , 2020.
- [4] Hatip, A., and Olgun, N., " On Refined Neutrosophic R-Module", *International Journal of Neutrosophic Science*, Vol. 7, pp.87-96, 2020.
- [5] Ibrahim, M.A., Agboola, A.A.A, Badmus, B.S., and Akinleye, S.A., "On Refined Neutrosophic Vector Spaces I", *International Journal of Neutrosophic Science*, Vol. 7, pp. 97-109, 2020.
- [6] P. Bedi, P. Gole and S. K. Agarwal, “18 Using deep learning for image-based plant disease detection”, *Internet of Things and Machine Learning in Agriculture*, pp. 369-402, 2021.
- [7] A. K. Dewangan, S. Kumar and T. B. Chandra, “Leaf-Rust and Nitrogen Deficient Wheat Plant Disease Classification using Combined Features and Optimized Ensemble Learning”, *Research Journal of Pharmacy and Technology*, Vol. 15, No. 6, pp. 2531-2538, 2022.
- [8] Y. Guo, J. Zhang, C. Yin, X. Hu, and Y. Zou et al., “Plant disease identification based on deep learning algorithm in smart farming”, *Discrete Dynamics in Nature and Society*, 2020.

- [9] S. Nandhini and K. Ashokkumar, "An automatic plant leaf disease identification using DenseNet-121 architecture with a mutation-based Henry gas solubility optimization algorithm", *Neural Computing and Applications*, Vol. 34, No. 7, pp. 5513-5534, 2022.
- [10] D. Aqel, S. A. Zubi, A. Mughaid, and Y. Jararweh, "Extreme learning machine for plant diseases classification: a sustainable approach for smart agriculture", *Cluster Computing*, Vol. 25, No. 3, pp. 2007-2020, 2022.
- [11] Khan, R.U., Khan, K., Albattah, W. and Qamar, A.M., 2021. Image-Based Detection of Plant Diseases: From Classical Machine Learning to Deep Learning Journey. *Wireless Communications and Mobile Computing*, 2021(1), p.5541859.
- [12] Habib, S., Alsanea, M., Aloraini, M., Al-Rawashdeh, H.S., Islam, M. and Khan, S., 2022. An efficient and effective deep learning-based model for real-time face mask detection. *Sensors*, 22(7), p.2602.
- [13] Albahli, S. and Nazir, T., 2023. A Circular Box-Based Deep Learning Model for the Identification of Signet Ring Cells from Histopathological Images. *Bioengineering*, 10(10), p.1147.
- [14] Albahli, S. and Nawaz, M., 2024. MedNet: Medical deepfakes detection using an improved deep learning approach. *Multimedia Tools and Applications*, 83(16), pp.48357-48375.
- [15] Wirtz, A., Mirashi, S.G. and Wesarg, S., 2018. Automatic teeth segmentation in panoramic X-ray images using a coupled shape model in combination with a neural network. In *Medical Image Computing and Computer Assisted Intervention—MICCAI 2018: 21st International Conference, Granada, Spain, September 16-20, 2018, Proceedings, Part IV 11* (pp. 712-719). Springer International Publishing.
- [16] Radočaj, P., Radočaj, D. and Martinović, G., 2024. Image-Based Leaf Disease Recognition Using Transfer Deep Learning with a Novel Versatile Optimization Module. *Big Data and Cognitive Computing*, 8(6), p.52.
- [17] Chug, A., Bhatia, A., Singh, A.P. and Singh, D., 2023. A novel framework for image-based plant disease detection using hybrid deep learning approach. *Soft Computing*, 27(18), pp.13613-13638.
- [18] Mao, R., Zhang, Y., Wang, Z., Hao, X., Zhu, T., Gao, S. and Hu, X., 2024. DAE-Mask: a novel deep-learning-based automatic detection model for in-field wheat diseases. *Precision Agriculture*, 25(2), pp.785-810.
- [19] Ullah, Z., Alsubaie, N., Jamjoom, M., Alajmani, S.H. and Saleem, F., 2023. EffiMob-Net: A deep learning-based hybrid model for detection and identification of tomato diseases using leaf images. *Agriculture*, 13(3), p.737.
- [20] Nawaz, M., Nazir, T., Javed, A., Amin, S.T., Jeribi, F. and Tahir, A., 2024. CoffeeNet: A deep learning approach for coffee plant leaves diseases recognition. *Expert Systems with Applications*, 237, p.121481.
- [21] Jerome, N.J., Jothiraj, S., Kandasamy, S., Ramachandran, D., Selvaraj, D. and Ilango, P., 2023. An effective approach for plant disease detection using assessment-based convolutional neural networks (A-CNN). *Journal of Advanced Research in Applied Sciences and Engineering Technology*, 31(3), pp.155-172.
- [22] Shah, A., Bangash, J.I., Khan, A.W., Ahmed, I., Khan, A., Khan, A. and Khan, A., 2022. Comparative analysis of median filter and its variants for removal of impulse noise from gray scale images. *Journal of King Saud University-Computer and Information Sciences*, 34(3), pp.505-519.
- [23] Cali, U., Deveci, M., Saha, S.S., Halden, U. and Smarandache, F., 2022. Prioritizing energy blockchain use cases using type-2 neutrosophic number-based EDAS. *Ieee Access*, 10, pp.34260-34276.
- [24] Saleh, I., Borhan, N., Yunus, A. and Rahiman, W., 2024. Comprehensive Technical Review of Recent Bio-Inspired Population-Based Optimization (BPO) Algorithms for Mobile Robot Path Planning. *IEEE Access*.
- [25] <https://www.kaggle.com/vipoooool/new-plant-diseases-dataset/data#>
- [26] Raja, D. and Karthikeyan, M., 2023. Red Deer Optimization with Deep Learning Enabled Agricultural Plant Disease Detection and Classification Model. *International Journal of Intelligent Engineering and Systems*, 16(5), pp.21-30.